

$F(R)$ gravity in the early Universe: Electroweak phase transition and chameleon mechanism

Taishi Katsuragawa,^a Shinya Matsuzaki^{b,c} and Eibun Senaha^d

^a*Institute of Astrophysics, Central China Normal University, Wuhan 430079, China*

^b*Center for Theoretical Physics and College of Physics, Jilin University, Changchun, 130012, China*

^c*Department of Physics, Nagoya University, Nagoya 464-8602, Japan*

^d*Center for Theoretical Physics of the Universe, Institute for Basic Science (IBS), Daejeon 34051, Korea*

E-mail: taishi@mail.ccnu.edu.cn, synya@jlu.edu.cn, senaha@ibs.re.kr

ABSTRACT: It is widely believed that the screening mechanism is an essential feature for the modified gravity theory. Although this mechanism has been examined thoroughly in the past decade, their analyses are based on the classical configuration of the matter fields. In this paper, we demonstrate a new formulation of the chameleon mechanism in $F(R)$ gravity theory, to shed light on quantum-field theoretical effects on the chameleon mechanism as well as the related scalaron physics, induced by the matter sector. We show a potential absence of the chameleon mechanism in the cosmic history based on a scale-invariant-extended scenario beyond the standard model of particle physics, in which a realistic electroweak phase transition, possibly yielding the right amount of baryon asymmetry of Universe today, simultaneously breaks the scale-invariance in the early Universe. Remarkably enough, the matter sector contribution to the trace of energy-momentum tensor turns out to be on the same order of magnitude as that computed in the classical perfect-fluid approximation, even though the theory involves the nontrivial electroweak-phase transition environment. We also briefly discuss the oscillation of the scalaron field and indirect generation of non-tensorial gravitational waves induced by the electroweak phase transition.

Contents

1	Introduction	1
2	$F(R)$ gravity and chameleon mechanism	3
2.1	Action and Weyl transformation	3
2.2	Effective potential and chameleon mechanism	5
2.3	Chameleon mechanism	5
3	EWPT in a SI-2HDM	7
3.1	A class of general SI-2HDM	7
3.2	The one-loop effective potential at zero temperature: EW symmetry breaking	9
3.3	The one-loop effective potential at finite temperature: EWPT	10
4	Chameleon mechanism over the EWPT	12
4.1	Scalaron in the EWPT environment	12
4.2	Trace of the energy-momentum tensor for SI-2HDM	13
4.3	Chameleon mechanism in the EWPT environment	14
4.4	Scalaron potential in the EWPT environment	15
5	Conclusion and Discussion	17

1 Introduction

Dark energy problem for the accelerated expansion of the Universe is one of the biggest mysteries in modern physics. Despite observational successes of the Λ CDM model in the framework of the general relativity, this model suffers from the cosmological constant problem, so the cosmological constant is still a phenomenological parameter. The modified gravity theories can provide us with alternative explanations for the dark energy, instead of ad hoc addition of the constant term. From the theoretical and phenomenological viewpoints, a variety of modified gravity theories has been proposed so far (for example, see [1, 2]), in which the new dynamics in the gravity sector is responsible for the origin of the late-time cosmological acceleration. Moreover, the challenges to test the beyond-standard in gravitational physics have received much attention [3–6].

In order for the modified gravity theory to be realized in nature, we need to open our eyes on the phenomenon at the smaller scale. Modifications for the cosmological scale also affect the predictions for galaxy clusters, galaxies, and the solar system, and they lead inconsistent results with the observations. Thus, we need to require the screening mechanism [7, 8] to restore the general relativity at certain scales, which suggests that the recovery of the general relativity must show the environment dependence.

The chameleon mechanism [9, 10] is one of the screening mechanisms, and it appears in the scalar-tensor theory and $F(R)$ gravity theory that include an extra scalar field. The potential term of the scalar field includes the coupling to the trace of energy-momentum tensor T^μ_μ which comprises the matter fields other than the scalar field itself. Trace of the energy-momentum tensor controls the mass of scalar field, which is very large in a high-density region at the local scale and very small in a low-density region at the cosmological scale. If the mass of the scalar field is large enough, the propagation, so-called the fifth force, is suppressed, and the modified gravity theories restore the general relativity.

It should be noted that the chameleon mechanism does not work if the trace of energy-momentum tensor vanishes. Such situations may arise in the early Universe because all species of particles are expected to become relativistic and behave as radiation. In the previous research by two of authors [11], the chameleon mechanism in the $F(R)$ gravity with the energy-momentum tensor which consists of the standard-model-particles was examined. It was found that the trace of energy-momentum tensor is proportional to the mass-squared and the temperature-squared, $T^\mu_\mu \propto m^2 T^2$, and that the chameleon mechanism remains to work in the high-temperature epoch. Note also that the previous analysis was based on the classical perfect-fluid approximation to construct the energy-momentum tensor.

Furthermore, towards the complete understanding for the cosmic history of the scalaron field, it is mandatory to take into account the thermal history of the matter sector. Thus, the formulation of the chameleon mechanism in the quantum field theory has a potential significance for the cosmology, which may give us a powerful tool to study the modified gravity in the early Universe. We also expect to find the unique phenomena related to the chameleon mechanism, which allows us to search the new physics originated from the modified gravity.

Actually, there is a crucial room to discuss the weakened or disabled chameleon mechanism in the early Universe, which was not evaluated in the previous work [11]: to our common knowledge in particle physics and cosmology, the electroweak phase transition (EWPT) is supposed to have taken place when the temperature dropped to the EW scale of $\mathcal{O}(100[\text{GeV}])$. If we believe the scale-invariance to be also broken by the EWPT through the dimensional transmutation in terms of quantum field theory, the potential of the scalar field receives a sudden and gigantic effect through the chameleon mechanism, as the trace of energy-momentum tensor changes from zero to nonzero. Note also that the perfect fluid approximation is expected to be no longer valid when the theory undergoes such a EWPT.

To address such a phase transition and check the above speculation, we thus need to construct the energy-momentum tensor based on the quantum field theory, and reproduce the scale-invariant epoch, where the trace of energy-momentum tensor vanishes, in the early Universe, by adopting a realistic scenario in the particle-physics side. Then one may simply expect the following phenomenon: during the scale-invariant epoch before the EWPT at higher temperature, the trace of the energy-momentum tensor is zero, and thus, the scalaron has a tiny mass before the EWPT. After the scale invariance is broken below the critical temperature (around the EW scale), the trace of energy-momentum tensor develops to become finite, and thus, the scalaron would dramatically acquire a large mass after the EWPT.

As a first and a brave step for such a completion of the chameleon mechanism in the early Universe, in this paper we discuss the scalaron dynamics coupled to a class of scale-invariant two-Higgs doublet model (SI-2HDM), chosen as a referenced realistic scenario in terms of thermal history in the early Universe. It has been shown in the SI-2HDM [12] that the thermal effect arising from the presence of heavy Higgs bosons with the masses around the EW scale (at the quantum loop level) successfully causes a strong first-order PT for the electroweak (EW) symmetry as well as for the scale symmetry. Moreover, if we do not impose a Z_2 parity on Yukawa sector, it is possible to have additional Yukawa couplings that induce the charge-conjugation and parity (CP) violation and/or flavor violation, which cannot be absorbed into the Cabibbo-Kobayashi-Maskawa matrix. As a result, a realistic amount of the baryon asymmetry of Universe (BAU) can be realized [13, 14] by the EW baryogenesis (EWBG) [15] (for reviews, see, *e.g.*, Refs. [16–19]), following the standard sphaleron-freeze out scenario coupled with a chiral/CP violating transport mechanism. Along such a cosmologically realistic scenario, we explicitly compute the energy-momentum tensor arising from the SI-2HDM matter sector and discuss the effect on the scalaron surrounded by the strong-first order EWPT environment in the early Universe. In particular, our main focus will be on the scalaron mass before and after the EWPT.

We also evaluate the time-evolution of the potential coupled with the SI-2HDM Lagrangian, motivated by the particle physics in the flat background, which is possible because the potential structure does not depend on the background of space-time, although several works [20, 21] had studied the time-evolution of the scalar field with the perfect-fluid approximation in the cosmological background. Strikingly enough, it is demonstrated that as far as order of magnitude evaluation for the trace of energy-momentum tensor (leading to the scalaron mass and the potential) is concerned, the perfect fluid approximation is actually valid even under this kind of nontrivial quantum dynamics having the EWPT.

We thus make a first attempt to evaluate the chameleon mechanism in the early Universe, explicitly based on the Lagrangian formalism. An indirect generation of non-tensorial gravitational waves induced by the strong-first order EWPT is also addressed. Though being somewhat specific to the choice of scenarios beyond the standard model of particle physics, what we provide in this paper involves the essential feature related to the PT for the scale symmetry breaking, which is applicable also to other similar models beyond the standard model.

2 $F(R)$ gravity and chameleon mechanism

In this section, we give a brief review of $F(R)$ gravity and chameleon mechanism for the scalar field. We also introduce the specific model of $F(R)$ gravity and its properties.

2.1 Action and Weyl transformation

The action of generic $F(R)$ gravity is given as follows:

$$S = \frac{1}{2\kappa^2} \int d^4x \sqrt{-g} F(R) + \int d^4x \sqrt{-g} \mathcal{L}_{\text{Matter}}[g^{\mu\nu}, \Phi], \quad (2.1)$$

where $F(R)$ is a function of the Ricci scalar R , and $\kappa^2 = 8\pi G = 1/M_{\text{pl}}^2$. M_{pl} is the reduced Planck mass $\sim 2 \times 10^{18} \text{[GeV]}$. $\mathcal{L}_{\text{Matter}}$ denotes the Lagrangian for a matter field Φ .

The variation with respect to the metric $g_{\mu\nu}$ leads to the equation of motion:

$$F_R(R)R_{\mu\nu} - \frac{1}{2}F(R)g_{\mu\nu} + (g_{\mu\nu}\square - \nabla_\mu\nabla_\nu)F_R(R) = \kappa^2 T_{\mu\nu}(g^{\mu\nu}, \Phi). \quad (2.2)$$

Here, $F_R(R)$ means the derivative of $F(R)$ with respect to R , $F_R(R) = \partial_R F(R)$, and the energy-momentum tensor $T_{\mu\nu}$ is given by

$$T_{\mu\nu}(g^{\mu\nu}, \Phi) = \frac{-2}{\sqrt{-g}} \frac{\delta(\sqrt{-g}\mathcal{L}_{\text{Matter}}(g^{\mu\nu}, \Phi))}{\delta g^{\mu\nu}}. \quad (2.3)$$

We can look into the dynamics of the new scalar field via the Weyl transformation. It is known that the $F(R)$ gravity is equivalent to the scalar-tensor theory via the Weyl transformation of the metric, which is the frame transformation from the Jordan frame $g_{\mu\nu}$ to the Einstein frame $\tilde{g}_{\mu\nu}$:

$$g_{\mu\nu} \rightarrow \tilde{g}_{\mu\nu} = e^{2\sqrt{1/6}\kappa\varphi} g_{\mu\nu} \equiv F_R(R)g_{\mu\nu}. \quad (2.4)$$

Under the Weyl transformation, the original action Eq. (2.1) is transformed as follows:

$$\begin{aligned} S = & \frac{1}{2\kappa^2} \int d^4x \sqrt{-\tilde{g}} \tilde{R} + \int d^4x \sqrt{-\tilde{g}} \left[-\frac{1}{2} \tilde{g}^{\mu\nu} (\partial_\mu\varphi)(\partial_\nu\varphi) - V_s(\varphi) \right] \\ & + \int d^4x \sqrt{-\tilde{g}} e^{-4\sqrt{1/6}\kappa\varphi} \mathcal{L}_{\text{Matter}} \left[e^{2\sqrt{1/6}\kappa\varphi} \tilde{g}^{\mu\nu}, \Phi \right]. \end{aligned} \quad (2.5)$$

We call $\varphi(x)$ the scalaron field and define its potential as,

$$V_s(\varphi) \equiv \frac{1}{2\kappa^2} \frac{RF_R(R) - F(R)}{F_R^2(R)}. \quad (2.6)$$

Note that through the Weyl transformation in Eq. (2.4), the Ricci scalar R is given as a function of the scalaron field φ , like $R = R(\varphi)$.

By the variation of the action in Eq. (2.5) with respect to the Einstein frame metric $\tilde{g}_{\mu\nu}$, we obtain the Einstein equation with the minimally coupled scalaron field. The variation with respect to the scalaron field φ gives us the equation of motion for the scalaron field,

$$0 = \sqrt{-\tilde{g}} \left[\tilde{\square}\varphi - \frac{\partial V_s(\varphi)}{\partial\varphi} \right] + \frac{\delta}{\delta\varphi} (\sqrt{-g}\mathcal{L}_{\text{Matter}}[g^{\mu\nu}, \Phi]). \quad (2.7)$$

Rewriting the second term in Eq. (2.7) with the relation between the metric and scalaron field,

$$\frac{\delta}{\delta\varphi} = \frac{2\kappa}{\sqrt{6}} g^{\mu\nu} \frac{\delta}{\delta g^{\mu\nu}}, \quad (2.8)$$

we obtain the equation of motion with respect to the scalaron field as

$$\tilde{\square}\varphi = \frac{\partial V_s(\varphi)}{\partial\varphi} + \frac{\kappa}{\sqrt{6}} e^{-4\sqrt{1/6}\kappa\varphi} T_\mu^\mu. \quad (2.9)$$

From Eq. (2.9), we define the effective potential of the scalaron field as follows:

$$V_{s\text{ eff.}}(\varphi) = V_s(\varphi) - \frac{1}{4}e^{-4\sqrt{1/6}\kappa\varphi}T_\mu^\mu. \quad (2.10)$$

We note that the effective potential of the scalaron includes the trace of energy-momentum tensor T_μ^μ . In other words, the matter distributions affect the potential structure of the scalaron, which leads the environment-dependent mass in the scalaron dynamics. This feature is related to so-called the chameleon mechanism, which we will see later in detail.

2.2 Effective potential and chameleon mechanism

Next, we discuss the minimum of the scalaron effective potential and the scalaron mass with the matter effect T_μ^μ . The first derivative of the scalaron effective potential is written in terms of the $F(R)$ function:

$$\frac{\partial V_{s\text{ eff.}}(\varphi)}{\partial \varphi} = \frac{1}{\sqrt{6}\kappa} \left(\frac{2F(R) - RF_R(R) + \kappa^2 T_\mu^\mu}{F_R^2(R)} \right). \quad (2.11)$$

The minimum of the potential at $\varphi = \varphi_{\min}$ should satisfy the stationary condition that Eq. (2.11) vanishes, which leads to

$$2F(R_{\min}) - R_{\min}F_R(R_{\min}) + \kappa^2 T_\mu^\mu = 0. \quad (2.12)$$

Note that R_{\min} is related to φ_{\min} through the Weyl transformation $e^{2\sqrt{1/6}\kappa\varphi_{\min}} = F_R(R_{\min})$.

Next, we evaluate the scalaron mass m_φ . The square of scalaron mass is defined as the value of the second derivative of the effective potential at the minimum. The second derivative of the effective potential is evaluated as follows:

$$\frac{\partial^2 V_{s\text{ eff.}}(\varphi)}{\partial \varphi^2} = \frac{1}{3F_{RR}(R)} \left(1 + \frac{RF_{RR}(R)}{F_R(R)} - \frac{2(2F(R) + \kappa^2 T_\mu^\mu)F_{RR}(R)}{F_R^2(R)} \right). \quad (2.13)$$

Substituting Eq. (2.12) into Eq. (2.13), we obtain

$$m_\varphi^2(T_\mu^\mu) = \frac{1}{3F_{RR}(R_{\min})} \left(1 - \frac{R_{\min}F_{RR}(R_{\min})}{F_R(R_{\min})} \right). \quad (2.14)$$

Note that since the stationary condition Eq. (2.12) determines φ_{\min} or R_{\min} , the scalaron mass changes according to the trace of the energy-momentum tensor T_μ^μ . If one can design the $F(R)$ function so that the scalaron mass becomes large enough in the high-density region, the scalaron is screened at the local scale.

2.3 Chameleon mechanism

Finally, we discuss the effect of the matter distribution to the scalaron mass. As an illustration, we consider the following model [22],

$$F(R) = R - \beta R_c \left[1 - \left(1 + \frac{R^2}{R_c^2} \right)^{-n} \right] + \alpha R^2. \quad (2.15)$$

The R_c is taken to be a typical energy scale, where the gravitational action deviates from the Einstein-Hilbert action, and one expects $R_c \sim \Lambda \simeq 4 \times 10^{-84} [\text{GeV}^2]$. The index n and the parameter β are chosen to be positive constants.

The α expresses another high energy scale. It has been known that the $F(R)$ gravity models for the dark energy generally suffer from the curvature singularity problem [23]. This problem can be cured with R^2 correction [24, 25], and the scalaron mass is upper-bounded and becomes finite in the high-density region [11, 26]. Note that R^2 term is not necessarily identified with the part of R^2 inflation model.

The curvature R should be larger than the dark energy scale R_c at the local scale. Therefore, we work in the large curvature limit $R_c < R$. In the large curvature limit, one can approximate Eq. (2.15) as

$$F(R) \approx R - \beta R_c + \beta R_c \left(\frac{R_c}{R} \right)^{2n} + \alpha R^2. \quad (2.16)$$

Here one could identify the βR_c as the cosmological constant, effectively. Then, the minimum of the potential is determined with Eq. (2.12)

$$0 = R - 2\beta R_c + 2(n+1)\beta R_c \left(\frac{R}{R_c} \right)^{-2n} + \kappa^2 T_\mu^\mu. \quad (2.17)$$

Note that the αR^2 does not affect the stationary condition. The second and third terms in Eq. (2.17) are negligible in the large curvature limit $R > R_c$, and one finds

$$R \approx -\kappa^2 T_\mu^\mu. \quad (2.18)$$

For the simplicity, we also assume that the matter contribution is approximately expressed as the pressure-less dust, $T_\mu^\mu = -\rho$, where ρ is the matter energy density. Then, the scalaron mass in Eq. (2.14) is evaluated in the large curvature limit as

$$m_\varphi^2(\rho) \approx \frac{R_c}{6n(2n+1)\beta} \left[\left(\frac{\kappa^2 \rho}{R_c} \right)^{-2(n+1)} + \frac{\alpha R_c}{n(2n+1)\beta} \right]^{-1} \frac{1}{1 + 2\alpha \kappa^2 \rho}. \quad (2.19)$$

We find that the scalaron mass is given by the increasing function of the energy density ρ , and thus, the scalaron becomes heavy in the high-density region of matter as we expected. This feature is called the chameleon mechanism which is one of the screening mechanism in the modified gravity. As a consequence, for example, the scalaron becomes heavy in the Solar System, where the scalaron field is screened, and the $F(R)$ gravity can be relevant to the observations. On the other hand, in the low-energy density environment, that is, on the cosmological scale, the scalaron field becomes dynamical dark energy.

Note that without R^2 term, the scalaron mass is given by

$$m_\varphi^2(\rho) \approx \frac{R_c}{6n(2n+1)\beta} \left(\frac{\kappa^2 \rho}{R_c} \right)^{2(n+1)}. \quad (2.20)$$

In this case, the scalaron mass is given by the monotonically increasing function of ρ and goes beyond the Planck mass at a certain energy density. On the other hand, in the limit

$R_c \ll R < 1/\alpha$ with R^2 correction, the scalaron mass approximately takes the constant value:

$$m_\varphi^2 \approx \frac{1}{6\alpha}. \quad (2.21)$$

Therefore, the scalaron mass is upper-bounded and characterized by the parameter α in the very high-density environment.

3 EWPT in a SI-2HDM

In this section, we consider a scale-invariant embedding for a scenario beyond the standard model of particle physics in the early Universe and compute the effective potential in the matter sector including the EWPT phenomenon, which will couple to the scalaron. As a reference scenario beyond the standard model, we shall take a class of general 2HDM, which has been shown to yield a realistic cosmic history including the realization of the right amount of BAU accompanied with a desired strong-first order EWPT [12–14]. In the present study, we shall apply such an EWBG scenario by extending it to be scale-invariant (general SI-2HDM).

3.1 A class of general SI-2HDM

We begin with introducing a general SI-2HDM, defined by the following Lagrangian:

$$\mathcal{L} = \mathcal{L}_{\text{2HDM}|_{\text{w/o } V_0}} - V_0(\Phi_1, \Phi_2), \quad (3.1)$$

where V_0 is the tree-level Higgs potential and the two Higgs doublets (Φ_1, Φ_2) are parametrized in terms of the fluctuation fields in the broken phase as

$$\Phi_i = \begin{pmatrix} \phi_i^+ \\ \frac{1}{\sqrt{2}}[v_i + h_i(x) + ia_i] \end{pmatrix}, \quad \text{for } i = 1, 2. \quad (3.2)$$

Their vacuum expectation values (VEVs) are characterized as $v_1 = v \cos \beta$ and $v_2 = v \sin \beta$, in which $v \simeq 246$ [GeV].

We work in the basis (“Higgs-Georgi basis”) where all the Nambu-Goldstone (NG) bosons do not show up in the physical Higgs spectra, and the only one Higgs doublet Φ_1 acquires the VEV $v \simeq 246$ [GeV]. Then the two Higgs doublet fields are transformed from those (Φ_1, Φ_2) in Eq.(3.2) by the orthogonal-basis rotation with the angle β into (H_1, H_2) like

$$\begin{aligned} H_1 &= \begin{pmatrix} G^+ \\ \frac{1}{\sqrt{2}}[v + h'_1 + iG^0] \end{pmatrix}, & H_2 &= \begin{pmatrix} H^+ \\ \frac{1}{\sqrt{2}}[v + h'_2 + iA] \end{pmatrix}, \\ \begin{pmatrix} h'_1 \\ h'_2 \end{pmatrix} &= \begin{pmatrix} c_\beta & s_\beta \\ -s_\beta & c_\beta \end{pmatrix} \begin{pmatrix} h_1 \\ h_2 \end{pmatrix}, \end{aligned} \quad (3.3)$$

where ($c_\beta \equiv \cos \beta$ and $s_\beta \equiv \sin \beta$) $G^{\pm,0}$ denote the NG boson fields to be eaten by W^\pm and Z . The neutral Higgs fields (h_1, h_2) will be further orthogonally rotated by an angle α to be mass eigenstate fields (h, H) in a similar manner.

The tree-level Higgs potential in the Higgs-Georgi basis is defined as

$$V_0(H_1, H_2) = \frac{\lambda_1}{2} (H_1^\dagger H_1)^2 + \frac{\lambda_2}{2} (H_2^\dagger H_2)^2 + \lambda_3 (H_1^\dagger H_1) (H_2^\dagger H_2) + \lambda_4 (H_1^\dagger H_2) (H_2^\dagger H_1) + \left\{ \frac{\lambda_5}{2} (H_1^\dagger H_2)^2 + [\lambda_6 (H_1^\dagger H_1) + \lambda_7 (H_2^\dagger H_2)] (H_1^\dagger H_2) + \text{h.c.} \right\}, \quad (3.4)$$

from which the tadpole conditions at tree-level are found to be

$$\frac{\lambda_1}{2} v^3 = 0, \quad \frac{\lambda_6}{2} v^3 = 0. \quad (3.5)$$

Therefore, for nonzero v , we find

$$\lambda_1 = \lambda_6 = 0, \quad V_0(v) = 0. \quad (3.6)$$

The masses of the charged Higgs H^\pm , CP-odd Higgs A , and CP-even Higgs (h, H) are evaluated as

$$\begin{aligned} m_{H^\pm}^2 &= \frac{\lambda_3}{2} v^2, & m_A^2 &= \frac{1}{2} (\lambda_3 + \lambda_4 - \lambda_5) v^2, \\ m_{\text{even}}^2 &\equiv \begin{pmatrix} m_h^2 & 0 \\ 0 & m_H^2 \end{pmatrix} = \begin{pmatrix} 0 & 0 \\ 0 & \frac{1}{2} (\lambda_3 + \lambda_4 + \lambda_5) v^2 \end{pmatrix} \end{aligned} \quad (3.7)$$

Note the presence of the massless neutral Higgs (h) in the mass matrix m_{even}^2 , which is called “*scalon*” [27] (not confused with scalaron) arising as the consequence of the classical-scale invariance in the present model. This massless *scalon* ensures the existence of a flat direction in the potential. We will investigate the EW symmetry breaking along this flat direction by assuming the *scalon*-Higgs mass to be zero at some renormalization scale.

Regarding the choice of the potential parameters, we may further assume the custodial symmetric limit, protecting the possibly sizable contribution to the ρ parameter, which is set as

$$m_{H^\pm}^2 = m_A^2, \quad (3.8)$$

and then, we obtain

$$\lambda_4 = \lambda_5 = \frac{m_H^2 - m_A^2}{v^2}. \quad (3.9)$$

In addition, we take $m_H = m_A$ for the benchmark point in addressing the EWPT and baryogenesis. In this case, we have

$$\lambda_3 = \frac{2m_H^2}{v^2}, \quad \lambda_4 = \lambda_5 = 0. \quad (3.10)$$

Finally, for the benchmark point where $m_H = m_A = m_{H^\pm}$ and $t_\beta \equiv \tan \beta = 1$, the Higgs potential in the present model is controlled only by the parameters λ_3 and λ_7 :

$$V_0(\phi) = \frac{\lambda_3}{2} (2\phi h + \phi^2) \left(H^+ H^- + \frac{1}{2} A^2 + \frac{1}{2} H^2 \right) - \lambda_7 \phi H \left(H^+ H^- + \frac{1}{2} A^2 + \frac{1}{2} H^2 \right), \quad (3.11)$$

where $\phi = \sqrt{\phi_1^2 + \phi_2^2}$ with ϕ_i being the constant background fields of the two Higgs doublets.

Note that as long as the effective potential for the background field ϕ is evaluated at the one-loop level, the second term with the coupling λ_7 in Eq. (3.11) does not contribute, so only the first term with the coupling λ_3 does, which will be replaced just by the heavy Higgs mass coupling (Eq.(3.10)), hence will be reduced merely to be the field-dependent (common) masses for the H, H^\pm and A , as will be seen in Eq.(3.13). Thus we can straightforwardly quote the result in the EWPT as well as the sphaleron freeze-out condition in [12], where the analyzed model has been set up in the scale-invariant limit, but not generic due to the requirement of a Z_2 symmetry among the two Higgs doublet fields. In particular, the numerical values listed in Table 1 of the reference can directly be applied even in the general 2HDM-setup, as we will see them in the next subsection. The only one exception is on estimation for the cutoff scale Λ regarding the present general SI-2HDM: one can compute the one-loop renormalization group equations for the potential couplings, and the explicit expressions, which are available in [28]. The straightforward one-loop computation thus tells us that the present model has a Landau pole (Λ_{LP}) at the scale $\simeq 8.8$ [TeV] (based on the Higgs-Georgi basis with the massless Higgs and other related inputs used in the later subsection being set at the renormalization scale $\tilde{\mu} = m_h (= 125$ [GeV])), which is somewhat larger than that in the SI-2HDM with the Z_2 symmetry imposed ($\Lambda_{LP} \simeq 6.3$ [TeV]) [12]. This is regarded as a cutoff scale up to which the present model is valid.

3.2 The one-loop effective potential at zero temperature: EW symmetry breaking

We follow the Gildener-Weinberg method [27] to compute the one-loop effective potential at zero temperature, $V_1(\phi)$, along the flat direction at tree-level. Note first that in the Gildener-Weinberg method, the NG bosons are exactly massless along the flat direction, hence do not contribute to the one-loop effective Higgs potential, or make the gauge-dependence left in the potential. ^{#1} Thus we can readily compute the one-loop effective potential by using the tree-level relation $\lambda_3 = 2m_H^2/v^2$ in Eq.(3.10) and the usual Yukawa and gauge interaction terms in the standard model to get

$$V_1(\phi) = \sum_{i=H,A,H^\pm,W^\pm,Z,t,b} n_i \frac{\tilde{m}(\phi)_i^4}{64\pi^2} \left(\log \frac{\tilde{m}_i^2(\phi)}{\tilde{\mu}^2} - c_i \right), \quad (3.12)$$

where n_i stands for the degree of freedom for each particle (note minus sign appears for fermion loops): $n_H = n_A = 1$, $n_{H^\pm} = 2$, $n_{W^\pm} = 6$, $n_Z = 3$, $n_t = n_b = -12$, and $c_i = 3/2$ (5/6) for scalars and fermions (gauge bosons), which come in the potential due to the $(\overline{\text{MS}})$ renormalization procedure at one-loop level. In Eq.(3.12), the $\tilde{m}(\phi)$ denotes the field-dependent masses for the heavy Higgses (H, A, H^\pm) and the standard model particles

^{#1}At finite temperature, however, the NG bosons get thermal masses, rendering the effective potential gauge dependent after thermal resummation [29] (see also Ref. [30]). Since there is no satisfactory gauge-invariant perturbative calculation method at present, we do not pursue this issue and take Landau gauge in our numerical analysis. In this gauge, the NG contributions are ϕ independent at leading order in resummed perturbation theory so that they do not appear in the following calculations.

(with being selected to be relatively heavy ones with the larger couplings to the ϕ , such as W^\pm, Z, t, b), defined by

$$\tilde{m}_i^2 = m_i^2 \frac{\phi^2}{v^2}. \quad (3.13)$$

Since the VEV v does not develop at the tree-level as the consequence of the classically scale-invariant setup, v emerges through the renormalization scale (μ) at the one-loop reflecting the dimensional transmutation (which is usually called radiative-EW breaking-mechanism). The tadpole condition at the one-loop level $\partial V_1(\phi)/\partial\phi = 0|_{\phi=v}$ leads to

$$\begin{aligned} v^2 &= \tilde{\mu}^2 \exp \left[-\frac{1}{2} - \frac{A}{B} \right], \\ A &= \sum_{i=H,A,H^\pm,W^\pm,Z,t,b} n_i \frac{\tilde{m}_i^4(\phi)}{64\pi^2 v^4} \left(\log \frac{\tilde{m}_i^2(\phi)}{v^2} - c_i \right), \\ B &= \sum_{i=H,A,H^\pm,W^\pm,Z,t,b} n_i \frac{\tilde{m}_i^4(\phi)}{64\pi^2 v^4}. \end{aligned} \quad (3.14)$$

Then the vacuum energy becomes

$$V_1(v) = -\frac{B}{2} v^4. \quad (3.15)$$

which has to be negative (i.e. $B > 0$ since $V_0(v) = 0$ along the flat direction) so as to realize the EW breaking at the true vacuum.

Eliminating the renormalization scale $\tilde{\mu}$ by using Eq.(3.14), the one-loop effective potential takes the form

$$V_1(\phi) = B\phi^4 \left(\log \frac{\phi^2}{v^2} - \frac{1}{2} \right), \quad (3.16)$$

and the 125 GeV Higgs mass is thus radiatively generated as

$$(125[\text{GeV}])^2 = m_h^2 = \left. \frac{\partial^2 V_1(\phi)}{\partial \phi^2} \right|_{\phi=v} = 8Bv^2. \quad (3.17)$$

3.3 The one-loop effective potential at finite temperature: EWPT

Including the finite temperature effect via the imaginary-time formalism and applying the resummation prescription [31–34], the one-loop potential Eq. (3.12) receives the corrections, and we obtain the effective potential $V_{h\text{ eff.}}(\phi, T)$:

$$\begin{aligned} V_{h\text{ eff.}}(\phi, T) &= \sum_{i=H,A,H^\pm,W_{L,T}^\pm,Z_{L,T},\gamma_L,t,b} n_i \left[\frac{\tilde{M}_i^4(\phi, T)}{64\pi^2} \left(\log \frac{\tilde{M}_i^2(\phi, T)}{\tilde{\mu}^2} - c_i \right) \right. \\ &\quad \left. + \frac{T^4}{2\pi^2} I_{B,F} \left(\frac{\tilde{M}_i^2(\phi, T)}{\tilde{\mu}^2} \right) \right], \end{aligned} \quad (3.18)$$

where $n_{W_{L(T)}} = 2(4)$, $n_{Z_{L(T)}} = 1(2)$, $c_{V_{L(T)}} = 3/2(1/2)$ ($V = W, Z$) and the field-dependent masses at the finite temperature $\tilde{M}_i^2(\phi, T)$ are given by

$$\tilde{M}_{H,A,H^\pm}^2(\phi, T) = \tilde{m}_{H,A,H^\pm}^2(\phi) + \Pi_{H,A,H^\pm}(T), \quad (3.19)$$

$$\tilde{M}_W^2(\phi, T) = \tilde{m}_W^2(\phi) + \Pi_W(T), \quad (3.20)$$

$$\begin{aligned} \tilde{M}_{Z_L,\gamma_L}^2(\phi, T) &= \frac{1}{2} \left[\frac{1}{4} (g_2^2 + g_1^2) \phi^2 + \Pi_W(T) + \Pi_B(T) \right. \\ &\quad \left. \pm \sqrt{\left(\frac{1}{4} (g_2^2 - g_1^2) \phi^2 + \Pi_W(T) - \Pi_B(T) \right)^2 + \frac{g_2^2 g_1^2}{4} \phi^4} \right], \quad (3.21) \end{aligned}$$

and for each field [35],

$$\Pi_{H,A,H^\pm}(T) = \frac{T^2}{12\pi^2 v^2} (6m_W^2 + 3m_Z^2 + 4m_H^2 + 6m_t^2 + 6m_b^2), \quad (3.22)$$

$$\Pi_W(T) = 2g_2^2 T^2, \quad (3.23)$$

$$\Pi_B(T) = 2g_1^2 T^2, \quad (3.24)$$

where g_2 and g_1 are the $SU(2)_L$ and $U(1)_Y$ couplings, respectively. For the other species, $\tilde{M}_i^2(\phi, T) = \tilde{m}_i^2(\phi)$. And, $I_{B,F}(\tilde{M}_i^2(\phi, T)/\tilde{\mu}^2)$ is defined by

$$I_{B,F}(a^2) = \int_0^\infty dx x^2 \log \left(1 \mp e^{-\sqrt{x^2+a^2}} \right), \quad (3.25)$$

where the minus sign is applied for bosons and the plus one for fermions. For the numerical evaluations of $I_{B,F}(a^2)$ and their derivatives with respect to a^2 , we employ fitting functions used in Ref. [36]. Their errors are small enough for our purpose.

With the effective potential in Eq. (3.18) at hand, we can analyze the EWPT and sphaleron freeze-out (after normalizing the effective potential to be 0 at $\phi = 0$, i.e., making a shift like $V(\phi, T) \rightarrow V(\phi, T) - V(\phi = 0, T)$). For successful EWBG, one has to satisfy $v/T > \xi_{\text{sph}}(T)$ at a transition temperature T (described below), where $\xi_{\text{sph}}(T)$ predominantly depends on sphaleron energy [37, 38]. We take $m_H^2 = m_A^2 = m_{H^\pm}^2 (= 382[\text{GeV}])^2$ [12] as the benchmark point. It turns out that all the results are the same as given in Table 1 of [12] (except for the cutoff scale around 10 [TeV], as noted in the previous subsection). Therefore, we can directly quote the successful benchmark parameters relevant to the strong first-order PT at the critical temperature (T_C) and the nucleation temperature for the EW-broken phase bubble (T_N) [12]:

$$\begin{aligned} v_C/T_C &= 211[\text{GeV}]/91.5[\text{GeV}] = 2.31, \quad \xi_{\text{sph}}(T_C) = 1.23, \\ v_N/T_N &= 229[\text{GeV}]/77.8[\text{GeV}] = 2.94, \quad \xi_{\text{sph}}(T_N) = 1.20, \quad E_{\text{cb}}(T_N)/T_N = 151.7, \quad (3.26) \end{aligned}$$

for $m_h = 125[\text{GeV}]$, $m_H = m_A = m_{H^\pm} = 382[\text{GeV}]$, and $t_\beta = 1$, where $v_{C/N}$ is the Higgs VEV at $T_{C(N)}$, $\xi_{\text{sph}}(T_{C(N)})$ denotes the related sphaleron decoupling parameter and $E_{\text{cb}}(T_N)$ represents the energy of the critical bubble (three-dimensional bounce action) [39].

In calculating ξ_{sph} , thermal effects on the sphaleron configuration are also taken into account. This is the reason why ξ_{sph} is slightly greater than a conventional rough criterion of $\xi_{\text{sph}} = 1$.

The parameter set listed in Eq.(3.26) makes it possible to accumulate the realistic amount of BAU, by introducing a moderate size of extra CP-violating Yukawa couplings in the top-charm sector [13] or bottom-strange sector [14]. Actually, the benchmark mass value for the heavy Higgses (382 [GeV]) is somewhat smaller than those adopted in [13] (500 [GeV]) and [14] (600 [GeV]), as well as the related quantities like T_C, T_N and so on. In evaluating the chiral/CP-violating transport process, however, the (coupled) diffusion rates and the thermal decay rates will not drastically get a significant effect from the mass difference in such a small range (unless extra colored particles are presented), though the (spatial) variation of $\tan \beta$ during the EWPT might slightly be altered. In that sense, the theoretical uncertainty in computing the BAU transported from the symmetric phase to the broken phase, through the flavor changing top-Yukawa or bottom Yukawa interaction, can be included at the same order of the size as that estimated in [13] or [14]. Keeping such possible uncertainties in our mind, we can roughly say that the plots in the parameter space drawn in figure 2 of [13] (for the case of top-transport scenario) or figures 1, 2 and 3 of [14] (for bottom-transport scenario) can be applied to our general SI-2HDM. One crucial difference is that since the so-called *alignment limit*, $\sin(\beta - \alpha) \rightarrow 1$, is naturally realized in the current model, our scenarios do not suffer from any severe experimental constraints such as the electric dipole moment of electron whose upper limit has been improved down to 1.1×10^{-29} [e cm] by ACME Collaboration [40].

4 Chameleon mechanism over the EWPT

In this section, we formulate the chameleon mechanism in the environment of the EWPT in the early Universe. Then, we apply it to the evaluation of the scalaron mass and potential in the EWPT environment, where the SI-2HDM plays a significant role as we introduced in the previous section.

4.1 Scalaron in the EWPT environment

To evaluate the scalaron mass in the environment of the EWPT epoch, we introduce the concept of thermal average to address the hot-and-dense environment. Since the scalaron couples with the matter sector through the trace of energy-momentum tensor, we consider a thermal average for the scalaron effective potential in Eq. (2.10). To study the thermal average for the scalaron, we postulate the following procedure for the scalaron effective potential:

$$\begin{aligned} \langle V_{s\text{ eff}}(\varphi) \rangle_{\text{thermal ave.}} &= \langle V_s(\varphi) \rangle_{\text{thermal ave.}} - \frac{1}{4} \left\langle e^{-4\sqrt{1/6}\kappa\varphi} \right\rangle_{\text{thermal ave.}} \langle T_\mu^\mu \rangle_{\text{thermal ave.}} \\ &= V_s(\varphi) - \frac{1}{4} e^{-4\sqrt{1/6}\kappa\varphi} \langle T_\mu^\mu \rangle_{\text{thermal ave.}} . \end{aligned} \quad (4.1)$$

In the first line of Eq. (4.1), we have used the fact that the scalaron decoupled from the thermal bath of the matter sector with the temperature T , due to the Planck-scale

suppression. The equality in the second line has been achieved because the gravity sector was also decoupled from the thermal bath at around the EWPT epoch of our interest. Thus, the effect of environment T_μ^μ on the scalaron mass can be evaluated as follows:

$$m_\varphi^2(T_\mu^\mu) = \frac{\partial^2}{\partial \varphi^2} \langle V_{\text{eff}}(\varphi) \rangle_{\text{thermal ave.}} . \quad (4.2)$$

Next, we address the method to compute the trace of the energy-momentum tensor based on the field-theoretical approaches. We can express the trace of the energy-momentum tensor by the scale transformation of the Lagrangian in the matter sector:

$$\begin{aligned} T_\mu^\mu &= \partial_\mu D^\mu = \delta_D \mathcal{L}_{\text{Matter}} \\ &= -\delta_D V_{\text{Matter}}, \end{aligned} \quad (4.3)$$

where D_μ denotes the dilatation current, and δ_D represents the operation of the infinitesimal scale (or dilatation) transformation. Here we have assumed a scale-invariant derivative coupling sector including the canonically normalized kinetic terms, so that the infinitesimal operation δ_D only extracts the potential term V_{Matter} . By inputting the matter Lagrangian in which one has interest into Eq. (4.3), we can evaluate the trace of energy-momentum, which does not rely on the classical perfect-fluid approximation.

4.2 Trace of the energy-momentum tensor for SI-2HDM

By incorporating the general SI-2HDM in the previous section into the targeted matter Lagrangian, we can evaluate the thermal average for T_μ^μ in Eq. (4.2) as

$$\langle T_\mu^\mu \rangle_{\text{thermal ave.}} = -\delta_D^\phi [V_{\text{eff}}(\phi, T)]|_{\phi=v(T)}, \quad (4.4)$$

where $V_{\text{eff}}(\phi, T)$ is given in Eq. (3.18), and δ_D^ϕ expresses the infinitesimal operator δ_D with respect to the Higgs field ϕ , which is constant in the space-time: $\delta_D^\phi \varphi = \varphi$. Eq. (4.4) can be computed as follows:

$$\begin{aligned} &\delta_D^\phi [V_{\text{eff}}(\phi, T)]|_{\phi=v(T)} \\ &= \sum_i n_i \tilde{m}_i^2(\phi) \left[\frac{\tilde{M}_i(\phi, T)}{16\pi^2} \left(\log \frac{\tilde{M}(\phi, T)_i^2(\phi)}{\tilde{\mu}^2} - c_i + \frac{1}{2} \right) \right. \\ &\quad \left. + \frac{T^4}{\pi^2} \frac{\partial}{\partial \tilde{M}_i^2(\phi, T)} I_{B,F} \left(\frac{\tilde{M}_i^2(\phi, T)}{\tilde{\mu}^2} \right) \right] \Big|_{\phi=v(T)} \\ &= \sum_i n_i \tilde{m}_i^2(\phi) \left[\frac{\tilde{M}_i^2(\phi, T)}{16\pi^2} \left(\log \frac{\tilde{M}(\phi, T)_i^2(\phi)}{\tilde{\mu}^2} - c_i + \frac{1}{2} \right) \right. \\ &\quad \left. + \frac{T^2}{2\pi^2} \int_0^\infty dx \frac{x}{\sqrt{x^2 + a^2}} \frac{1}{\exp[\sqrt{x^2 + a^2}] \mp 1} \right] \Big|_{a^2 = \tilde{M}^2(v(T), T)/T^2} \\ &= \sum_i n_i \tilde{m}_i^2(\phi) \frac{\tilde{M}_i^2(\phi, T)}{16\pi^2} \left(\log \frac{\tilde{M}(\phi, T)_i^2(\phi)}{\tilde{\mu}^2} - c_i + \frac{1}{2} \right) + (\rho - 3p)|_{a^2 = \tilde{M}^2(v(T), T)/T^2} . \quad (4.5) \end{aligned}$$

Here the temperature dependence of the Higgs VEV, $v(T)$, is completely determined by the potential analysis in the previous section.

It is remarkable that the second term in the final line of Eq. (4.5) is corresponding to the trace of energy-momentum tensor for the perfect fluid, while the first term gives the deviation from the perfect fluid approximation arising from the SI-2HDM as a quantum field theory. One can easily check that at $\phi = 0$ the left-hand-side of Eq.(4.5) goes to zero, reflecting the restoration of the scale invariance as well as the EW symmetry, which will more clearly be observed later soon.

4.3 Chameleon mechanism in the EWPT environment

When we evaluate the trace of energy-momentum tensor in SI-2HDM based on Eq. (4.5) with respect to the temperature T , we obtain the plot in Fig. 1. We evaluated the

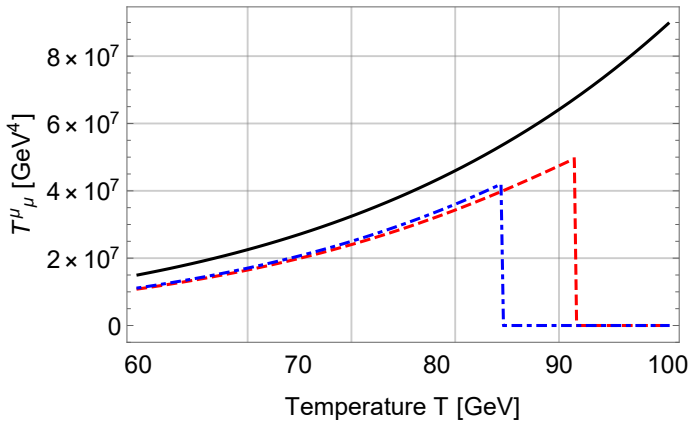


Figure 1. The dashed red and dot-dashed blue lines show the trace of the energy-momentum tensor with (without) resummation prescription, respectively. The solid black line shows the trace of the energy-momentum tensor constructed only from the standard-model-particles with the perfect-fluid approximation. The coincidence in magnitude between the solid black and other curves imply the validity of the approximation and the thermal decoupling of heavier Higgses with the mass above 100 [GeV].

temperature-dependence of the trace of energy-momentum tensor in the SI-2HDM in two different ways (the dashed red and dot-dashed blue lines) to take into account the resummation prescription. In both two cases, the SI-2HDM model predicts a sharp dump at around 80–90[GeV], which indeed reflects the strong-first order EWPT, and the trace of energy-momentum tensor becomes zero as we expected. We also plot the case with perfect fluid comprised only by the standard model particles (the solid black line).

The Fig. 1 clearly demonstrates that the SI-2HDM with the exact analysis based on the quantum field theory does not show a large deviation from the perfect-fluid approximation in the trace of energy-momentum tensor, though they are somewhat different by order one factor. Thus, it has been shown that the perfect-fluid approximation actually works appropriately in the evaluation of the chameleon mechanism, although it cannot describe the EWPT.

Next, we convert the trace of energy-momentum tensor as in Fig. 1 into the temperature-dependence of the scalaron mass. We show the result in Fig. 2. As an illustration, we take

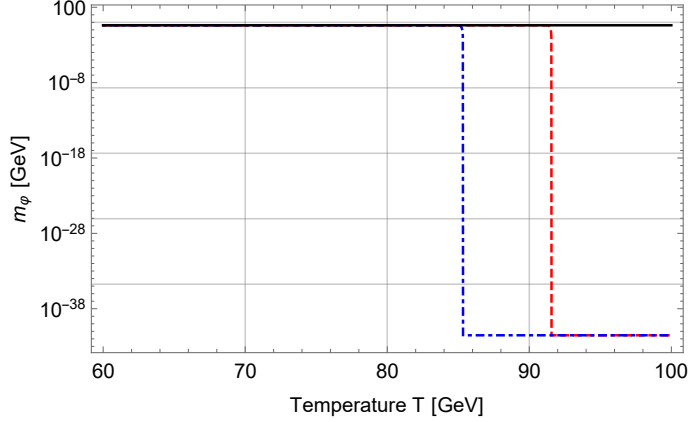


Figure 2. The dashed red and dot-dashed blue lines show the scalaron mass for SI-2HDM with (without) resummation prescription, respectively. The solid black line shows the scalaron mass for the perfect-fluid approximation. The parameters of the $F(R)$ function are chosen as $n = 1$, $\beta = 2$, $\alpha = 1[\text{GeV}^{-2}]$. The coincidence is seen between the perfect-fluid approximation and the SI-2HDM as the quantum field theory, in the same way as described in Fig. 1.

the parameters in Eq. (2.15) as $n = 1$, $\beta = 2$, $\alpha = 1[\text{GeV}^{-2}]$. Since the trace of energy-momentum tensor is zero before the EWPT, the dashed red and dot-dashed blue lines show that the scalaron mass is given by the dark energy scale, $m_\varphi \sim 3 \times 10^{-33}[\text{eV}]$. After the EWPT, the effective potential of scalaron achieve the finite trace of energy-momentum tensor, and the chameleon mechanism makes the scalaron mass heavy. The scalaron mass after the EWPT takes the constant value, $m_\varphi \sim 0.1[\text{GeV}]$, for the choice of $\alpha = 1[\text{GeV}^{-2}]$. On the other hand, the scalaron mass in the case of perfect fluid keeps constant as in [11].

4.4 Scalaron potential in the EWPT environment

Finally, we discuss the scalaron potential over the EWPT environment created from the SI-2HDM. We consider the effective potential of the scalaron field before and after the EWPT. Right after the EWPT ($T \lesssim T_C \simeq 91.5$ [GeV]) with and without the resummation prescription, the trace of energy-momentum tensor keeps almost a constant value (See Fig. 1). Hence, by inputting $T_\mu^\mu = 0[\text{GeV}^4]$ and $T_\mu^\mu \sim 4 \times 10^7[\text{GeV}^4]$, we plot the form of the effective potential before and after the EWPT, given in Figs. 3 and 4.

In this analysis, we set $\alpha = 10^{22}[\text{GeV}^{-2}]$, which corresponds to the experimental upper-bound from the fifth forth experiment [41]. Before the EWPT ($T \gtrsim T_C$), the effective potential does not receive the effect of the chameleon mechanism because the trace of energy-momentum tensor vanishes. Then, the potential minimum locates at around $\kappa\varphi \sim -0.1$. Immediately after the EWPT ($T \lesssim T_C$), the chameleon mechanism starts to work due to the non-zero trace of energy-momentum tensor induced by the radiative breaking of the scale and EW symmetries, and the effective potential is lifted by the SI-2HDM-matter contributions. Then, the potential minimum locates at around $\kappa\varphi \sim 0$.

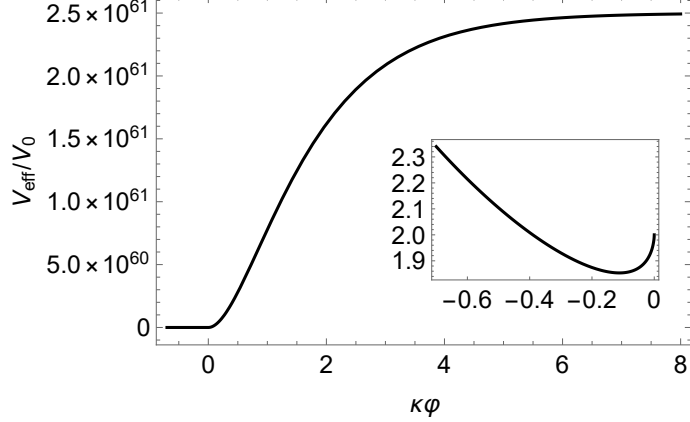


Figure 3. The solid black line shows the effective potential of the scalar field with $n = 1$, $\beta = 2$, and $\alpha = 10^{22}[\text{GeV}^{-2}]$. The potential is normalized by $V_0 = \frac{R_c}{2\kappa^2} \sim \rho_\Lambda$. Before the EWPT, the SI-2HDM does not generate the trace of energy-momentum tensor, and thus, the chameleon mechanism does not work.

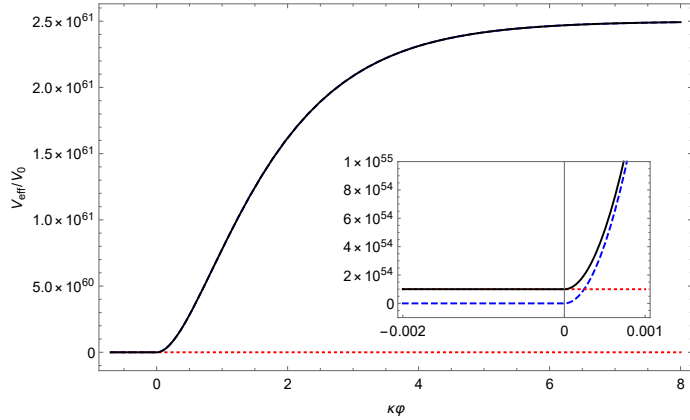


Figure 4. The same parameter choice as in Fig. 3. The solid black line shows the effective potential although the blue dashed line represents the original potential of the scalaron field. The red dotted line shows the matter contribution. After the EWPT, the trace of energy-momentum tensor takes the non-zero value, and affects the effective potential due to the chameleon mechanism. Immediate the EWPT, $T_\mu^\mu \sim 4 \times 10^7[\text{GeV}^4]$.

From the potential analysis, we can conjecture the new thermal history of the scalaron field with taking into account the EWPT; the scalaron field at the original potential minimum is pushed away from the minimum by the EWPT via the chameleon mechanism, and the scalaron field would locate around the new potential minimum. As the Universe expands, the matter effect is decreasing in the effective potential, and the potential form is approaching to the original one.

The above scenario gives the nonperturbative effect to the time-evolution of the scalaron field, and the behavior of the scalaron field after the EWPT is nontrivial, but expected to be around the potential minimum. We exaggerate that the above phenomenon is driven by the quantum effect in the matter sector, which we cannot observe in the perfect-fluid

approximation.

5 Conclusion and Discussion

We have investigated the chameleon mechanism in the early Universe, especially the EWPT epoch, with the formulation based on the quantum field theory. We have utilized a class of general SI-2HDM to describe the EWPT and evaluated the trace of energy-momentum tensor. The formulation of the chameleon mechanism in the analytic manner has shown the correspondence to the classical perfect-fluid approximation. By interpolating the numerical results, we have confirmed that as far as the order of magnitude is concerned, the trace of energy-momentum tensor constructed in the SI-2HDM shows almost the same temperature-dependence as that in the perfect fluid approximation. Moreover, we have converted the temperature-dependence of the trace of the energy-momentum tensor into the that of the scalaron mass, to find that the scalaron has tiny mass comparable to the dark energy scale, $m_\varphi \sim 10^{-33}[\text{eV}]$, due to the absence of the chameleon mechanism before the EWPT. This is reflected by the drastic change of the scalaron potential caused by the suddenly increased trace of energy-momentum tensor as we have shown the shape of the scalaron potential before and after the EWPT.

A couple of comments and discussions on future prospects regarding what we have clarified in the present paper are as follows. Two of authors have studied the scenario that the scalaron can be dark matter [42]. When we quantize the excitation or perturbation around the potential minimum of the scalaron field, we have the particle picture of the scalaron field. This scenario relies on the assumption that the scalaron field keeps the harmonic oscillation to act as a dust in the cosmic history, and thus, the initial condition for the oscillation seemed to be given by hand in analogy with the harmonic oscillation of the axion dark matter.

Regarding the origin of the harmonic oscillation, we could find the species of the oscillation in the present paper. For the scalaron, the matter sector works as an external field, and the scalaron field would receive the nonlinear effect to start the forced oscillation when the external field suddenly changes. Because the EWPT in the matter sector “kicks” the scalaron field through the chameleon mechanism, we can expect that such a kick generates the harmonic oscillation of the scalaron field. We also expect that the initial condition for the scalaron field at the original potential minimum would be wiped out by the matter effect, to avoid the fine-tuning for the harmonic oscillation of the scalaron.

The kick solution had been already argued in [20, 21]. This is induced by the comparison to the Hubble friction term in the cosmological background, which causes the continuous change of potential form. On the other hand, the kick by the EWPT is not the continuous one, and thus, we can conclude that we have found another possibility of the kick solution in the early Universe. We also emphasize that the PT does not happen in the scalaron sector because the scalaron field decouples from the thermal equilibrium due to the Planck-suppressed couplings to the other fields. Thus, the discrete change of the potential shape in the chameleon sector should be regarded as a transition-like phenomena induced by the genuine EWPT in the matter sector.

In relation to the oscillation of the scalaron, we might find the intriguing effect in the phenomenology. As we have mentioned, the EWPT deforms the potential shape of the scalaron field, which may generate the oscillation of the scalaron field. Since the scalaron field originates from the gravity sector through the Weyl transformation, the oscillation of the scalaron field would imply generation of an intrinsic gravitational wave. It has been suggested that the $F(R)$ gravity predicts the scalar mode of the gravitational waves [43, 44], which is described by the fluctuation of the scalaron field around the potential minimum. Therefore, we may expect the origin of the non-tensorial polarization of the gravitational waves induced by the EWPT. Besides the well-known fact that a strong-first order PT can directly generate the gravitational waves [45–48], our analysis gives another insight in that the EWPT could indirectly generate the scalar mode of the gravitational waves in the $F(R)$ gravity. This speculation would open the brand-new phenomenology to explore the beyond-standard-physics in both particle and gravitational physics.

Acknowledgments

T.K. is supported by International Postdoctoral Exchange Fellowship Program at Central China Normal University and Project funded by China Postdoctoral Science Foundation 2018M632895. S.M. is supported in part by the JSPS Grant-in-Aid for Young Scientists (B) No. 15K17645 and the Seeds Funding of Jilin University. E.S. is supported by IBS under the project code, IBS-R018-D1.

References

- [1] T. Clifton, P. G. Ferreira, A. Padilla, and C. Skordis, “Modified Gravity and Cosmology,” *Phys. Rept.* **513** (2012) 1–189, [arXiv:1106.2476 \[astro-ph.CO\]](https://arxiv.org/abs/1106.2476).
- [2] S. Nojiri and S. D. Odintsov, “Unified cosmic history in modified gravity: from $F(R)$ theory to Lorentz non-invariant models,” *Phys. Rept.* **505** (2011) 59–144, [arXiv:1011.0544 \[gr-qc\]](https://arxiv.org/abs/1011.0544).
- [3] A. Joyce, B. Jain, J. Khoury, and M. Trodden, “Beyond the Cosmological Standard Model,” *Phys. Rept.* **568** (2015) 1–98, [arXiv:1407.0059 \[astro-ph.CO\]](https://arxiv.org/abs/1407.0059).
- [4] E. Berti *et al.*, “Testing General Relativity with Present and Future Astrophysical Observations,” *Class. Quant. Grav.* **32** (2015) 243001, [arXiv:1501.07274 \[gr-qc\]](https://arxiv.org/abs/1501.07274).
- [5] K. Koyama, “Cosmological Tests of Modified Gravity,” *Rept. Prog. Phys.* **79** no. 4, (2016) 046902, [arXiv:1504.04623 \[astro-ph.CO\]](https://arxiv.org/abs/1504.04623).
- [6] P. Bull *et al.*, “Beyond Λ CDM: Problems, solutions, and the road ahead,” *Phys. Dark Univ.* **12** (2016) 56–99, [arXiv:1512.05356 \[astro-ph.CO\]](https://arxiv.org/abs/1512.05356).
- [7] P. Brax, “Screening mechanisms in modified gravity,” *Class. Quant. Grav.* **30** (2013) 214005.
- [8] C. Burrage and J. Sakstein, “Tests of Chameleon Gravity,” *Living Rev. Rel.* **21** no. 1, (2018) 1, [arXiv:1709.09071 \[astro-ph.CO\]](https://arxiv.org/abs/1709.09071).
- [9] J. Khoury and A. Weltman, “Chameleon fields: Awaiting surprises for tests of gravity in space,” *Phys. Rev. Lett.* **93** (2004) 171104, [arXiv:astro-ph/0309300 \[astro-ph\]](https://arxiv.org/abs/astro-ph/0309300).

[10] J. Khoury and A. Weltman, “Chameleon cosmology,” *Phys. Rev. D* **69** (2004) 044026, [arXiv:astro-ph/0309411 \[astro-ph\]](https://arxiv.org/abs/astro-ph/0309411).

[11] T. Katsuragawa and S. Matsuzaki, “Cosmic History of Chameleonic Dark Matter in $F(R)$ Gravity,” *Phys. Rev. D* **97** no. 6, (2018) 064037, [arXiv:1708.08702 \[gr-qc\]](https://arxiv.org/abs/1708.08702). [Erratum: Phys. Rev. D97,no.12,129902(2018)].

[12] K. Fuyuto and E. Senaha, “Sphaleron and critical bubble in the scale invariant two Higgs doublet model,” *Phys. Lett. B* **747** (2015) 152–157.

[13] K. Fuyuto, W.-S. Hou, and E. Senaha, “Electroweak baryogenesis driven by extra top Yukawa couplings,” *Phys. Lett. B* **776** (2018) 402–406, [arXiv:1705.05034 \[hep-ph\]](https://arxiv.org/abs/1705.05034).

[14] T. Modak and E. Senaha, “Electroweak baryogenesis via bottom transport,” [arXiv:1811.08088 \[hep-ph\]](https://arxiv.org/abs/1811.08088).

[15] V. A. Kuzmin, V. A. Rubakov, and M. E. Shaposhnikov, “On the Anomalous Electroweak Baryon Number Nonconservation in the Early Universe,” *Phys. Lett. 155B* (1985) 36.

[16] M. Quiros, “Field theory at finite temperature and phase transitions,” *Helv. Phys. Acta* **67** (1994) 451–583.

[17] V. A. Rubakov and M. E. Shaposhnikov, “Electroweak baryon number nonconservation in the early universe and in high-energy collisions,” *Usp. Fiz. Nauk* **166** (1996) 493–537, [arXiv:hep-ph/9603208 \[hep-ph\]](https://arxiv.org/abs/hep-ph/9603208). [Phys. Usp.39,461(1996)].

[18] K. Funakubo, “CP violation and baryogenesis at the electroweak phase transition,” *Prog. Theor. Phys.* **96** (1996) 475–520, [arXiv:hep-ph/9608358 \[hep-ph\]](https://arxiv.org/abs/hep-ph/9608358).

[19] D. E. Morrissey and M. J. Ramsey-Musolf, “Electroweak baryogenesis,” *New J. Phys.* **14** (2012) 125003, [arXiv:1206.2942 \[hep-ph\]](https://arxiv.org/abs/1206.2942).

[20] P. Brax, C. van de Bruck, A.-C. Davis, J. Khoury, and A. Weltman, “Detecting dark energy in orbit - The Cosmological chameleon,” *Phys. Rev. D* **70** (2004) 123518, [arXiv:astro-ph/0408415 \[astro-ph\]](https://arxiv.org/abs/astro-ph/0408415).

[21] A. L. Erickcek, N. Barnaby, C. Burrage, and Z. Huang, “Catastrophic Consequences of Kicking the Chameleon,” *Phys. Rev. Lett.* **110** (2013) 171101, [arXiv:1304.0009 \[astro-ph.CO\]](https://arxiv.org/abs/1304.0009).

[22] A. A. Starobinsky, “Disappearing cosmological constant in $f(R)$ gravity,” *JETP Lett.* **86** (2007) 157–163, [arXiv:0706.2041 \[astro-ph\]](https://arxiv.org/abs/0706.2041).

[23] A. V. Frolov, “A Singularity Problem with $f(R)$ Dark Energy,” *Phys. Rev. Lett.* **101** (2008) 061103, [arXiv:0803.2500 \[astro-ph\]](https://arxiv.org/abs/0803.2500).

[24] A. Dev, D. Jain, S. Jhingan, S. Nojiri, M. Sami, and I. Thongkool, “Delicate $f(R)$ gravity models with disappearing cosmological constant and observational constraints on the model parameters,” *Phys. Rev. D* **78** (2008) 083515, [arXiv:0807.3445 \[hep-th\]](https://arxiv.org/abs/0807.3445).

[25] T. Kobayashi and K.-i. Maeda, “Can higher curvature corrections cure the singularity problem in $f(R)$ gravity?,” *Phys. Rev. D* **79** (2009) 024009, [arXiv:0810.5664 \[astro-ph\]](https://arxiv.org/abs/0810.5664).

[26] I. Thongkool, M. Sami, R. Gannouji, and S. Jhingan, “Constraining $f(R)$ gravity models with disappearing cosmological constant,” *Phys. Rev. D* **80** (2009) 043523, [arXiv:0906.2460 \[hep-th\]](https://arxiv.org/abs/0906.2460).

[27] E. Gildener and S. Weinberg, “Symmetry Breaking and Scalar Bosons,” *Phys. Rev. D* **13** (1976) 3333.

[28] G. C. Branco, P. M. Ferreira, L. Lavoura, M. N. Rebelo, M. Sher, and J. P. Silva, “Theory and phenomenology of two-Higgs-doublet models,” *Phys. Rept.* **516** (2012) 1–102, [arXiv:1106.0034 \[hep-ph\]](https://arxiv.org/abs/1106.0034).

[29] C.-W. Chiang and E. Senaha, “On gauge dependence of gravitational waves from a first-order phase transition in classical scale-invariant $U(1)'$ models,” *Phys. Lett. B* **774** (2017) 489–493, [arXiv:1707.06765 \[hep-ph\]](https://arxiv.org/abs/1707.06765).

[30] H. H. Patel and M. J. Ramsey-Musolf, “Baryon Washout, Electroweak Phase Transition, and Perturbation Theory,” *JHEP* **07** (2011) 029, [arXiv:1101.4665 \[hep-ph\]](https://arxiv.org/abs/1101.4665).

[31] R. R. Parwani, “Resummation in a hot scalar field theory,” *Phys. Rev. D* **45** (1992) 4695, [arXiv:hep-ph/9204216 \[hep-ph\]](https://arxiv.org/abs/hep-ph/9204216). [Erratum: Phys. Rev. D48,5965(1993)].

[32] W. Buchmuller, T. Helbig, and D. Walliser, “First order phase transitions in scalar electrodynamics,” *Nucl. Phys. B* **407** (1993) 387–411.

[33] S. Chiku and T. Hatsuda, “Optimized perturbation theory at finite temperature,” *Phys. Rev. D* **58** (1998) 076001, [arXiv:hep-ph/9803226 \[hep-ph\]](https://arxiv.org/abs/hep-ph/9803226).

[34] K. Funakubo and E. Senaha, “Two-loop effective potential, thermal resummation, and first-order phase transitions: Beyond the high-temperature expansion,” *Phys. Rev. D* **87** no. 5, (2013) 054003, [arXiv:1210.1737 \[hep-ph\]](https://arxiv.org/abs/1210.1737).

[35] M. E. Carrington, “The Effective potential at finite temperature in the Standard Model,” *Phys. Rev. D* **45** (1992) 2933–2944.

[36] K. Funakubo and E. Senaha, “Electroweak phase transition, critical bubbles and sphaleron decoupling condition in the MSSM,” *Phys. Rev. D* **79** (2009) 115024, [arXiv:0905.2022 \[hep-ph\]](https://arxiv.org/abs/0905.2022).

[37] N. S. Manton, “Topology in the Weinberg-Salam Theory,” *Phys. Rev. D* **28** (1983) 2019.

[38] F. R. Klinkhamer and N. S. Manton, “A Saddle Point Solution in the Weinberg-Salam Theory,” *Phys. Rev. D* **30** (1984) 2212.

[39] A. D. Linde, “Decay of the False Vacuum at Finite Temperature,” *Nucl. Phys. B* **216** (1983) 421. [Erratum: Nucl. Phys.B223,544(1983)].

[40] ACME Collaboration, V. Andreev *et al.*, “Improved limit on the electric dipole moment of the electron,” *Nature* **562** no. 7727, (2018) 355–360.

[41] J. A. R. Cembranos, “Dark Matter from R2-gravity,” *Phys. Rev. Lett.* **102** (2009) 141301, [arXiv:0809.1653 \[hep-ph\]](https://arxiv.org/abs/0809.1653).

[42] T. Katsuragawa and S. Matsuzaki, “Dark matter in modified gravity?,” *Phys. Rev. D* **95** no. 4, (2017) 044040, [arXiv:1610.01016 \[gr-qc\]](https://arxiv.org/abs/1610.01016).

[43] C. Corda, “An oscillating Universe from the linearized R^2 theory of gravity,” *Gen. Rel. Grav.* **40** (2008) 2201–2212, [arXiv:0802.2523 \[astro-ph\]](https://arxiv.org/abs/0802.2523).

[44] S. Capozziello, C. Corda, and M. F. De Laurentis, “Massive gravitational waves from $f(R)$ theories of gravity: Potential detection with LISA,” *Phys. Lett. B* **669** (2008) 255–259, [arXiv:0812.2272 \[astro-ph\]](https://arxiv.org/abs/0812.2272).

[45] A. Kosowsky, M. S. Turner, and R. Watkins, “Gravitational radiation from colliding vacuum bubbles,” *Phys. Rev. D* **45** (1992) 4514–4535.

[46] A. Kosowsky, M. S. Turner, and R. Watkins, “Gravitational waves from first order cosmological phase transitions,” *Phys. Rev. Lett.* **69** (1992) 2026–2029.

- [47] A. Kosowsky and M. S. Turner, “Gravitational radiation from colliding vacuum bubbles: envelope approximation to many bubble collisions,” *Phys. Rev.* **D47** (1993) 4372–4391, [arXiv:astro-ph/9211004 \[astro-ph\]](https://arxiv.org/abs/astro-ph/9211004).
- [48] M. Kamionkowski, A. Kosowsky, and M. S. Turner, “Gravitational radiation from first order phase transitions,” *Phys. Rev.* **D49** (1994) 2837–2851, [arXiv:astro-ph/9310044 \[astro-ph\]](https://arxiv.org/abs/astro-ph/9310044).